ISSN 2072-5981

Magnetic Resonance in Solids

Electronic Journal

Volume **15, 2013**
No. **1, 13101** – *7 pages*

http://mrsej.ksu.ru

Established and published by Kazan University
Sponsored by International Society of Magnetic Resonance (ISMAR)
Registered by Russian Federation Committee on Press, August 2, 1996
First Issue was appeared at July 25, 1997

"***Magnetic Resonance in Solids. Electronic Journal***" (**MRS*ej***) is a peer-reviewed, all electronic journal, publishing articles which meet the highest standards of scientific quality in the field of basic research of a magnetic resonance in solids and related phenomena. **MRS*ej*** is free for the authors (no page charges) as well as for the readers (no subscription fee). The language of **MRS*ej*** is English. All exchanges of information will take place via Internet. Articles are submitted in electronic form and the refereeing process uses electronic mail. All accepted articles are immediately published by being made publicly available by Internet (http://**MRS*ej***.ksu.ru).

* In Kazan University the Electron Paramagnetic Resonance (EPR) was discovered by Zavoisky E.K. in 1944.

A novel data on Ag_5SbS_4 and $CuPbSbS_3$ probed by antimony NQR spectroscopy†

A.Yu. Orlova [1,] *, R.R. Gainov [1], A.V. Dooglav [1], I.N. Pen'kov [2]

[1] Institute of Physics, Kazan Federal University, Kremlevskaya, 18, Kazan 420008, Russia

[2] Institute of Geology and Petroleum Technologies, Kazan Federal University, Kremlevskaya, 18, Kazan 420008, Russia

E-mail: AnnaYuOrlova@gmail.com

(Received December 13, 2012; accepted January 10, 2013)

Investigations of Sb-based chalcogenides, stephanite Ag_5SbS_4 and bournonite $CuPbSbS_3$, have been performed by ^{121,123}Sb nuclear quadrupole resonance (NQR). In stephanite a phase transition at 140 K and internal diffusion motions with an activation energy of 0.29 eV have been experimentally detected. The analysis of experimental results for bournonite revealed two crystal-chemical positions of Sb in the unit cell with distinct local symmetry. The NQR frequencies ν and line-widths $\Delta\nu$ data indicate that $Sb(A)S_3$ complex has almost axial symmetry, but $Sb(B)S_3$ complex is substantially distorted.

PACS: 76.60.Gv, 91.60.Ed, 91.60.Tn.

Keywords: NQR spectroscopy, chalcogenides, stephanite, bournonite, crystal chemistry, transport properties

1. Introduction

Multicomponent silver and copper chalcogenides have received much attention during recent years due to their important technological applications. These compounds have intriguing optical, electric and ferroelectric properties, as well as ionic conductivity, etc. [1, 2]. To explain physical properties of chalcogenides an exact knowledge of the crystal structure of solids state materials is necessary. In many cases NQR spectroscopy provides detailed information about static and dynamic properties of solids. NQR spectroscopy employs nuclei having a quadrupole moment, such as Cu, Na, Co, As, Sb, Bi, and others [3, 4]. NQR experimental results and their analysis highlight the details of ionic arrangement, phase-structural transformations, exchange interactions, internal movements, etc. [5].

In this report we present some results of investigations of two complex sulfides: stephanite Ag_5SbS_4 and bournonite $CuPbSbS_3$ by ^{121,123}Sb NQR.

2. Crystal structure

The common feature of the studied chalcogenides is a complex composite structure based on isolated pyramidal groups of SbS_3. Stephanite, Ag_5SbS_4, has the centered orthorhombic unit cell with space group symmetry $Cmc2_1$ and contains single Sb atom, forming the SbS_3 pyramids (Fig. 1). The SbS_3 pyramids are connected only via Ag atoms [6]. In contrast to stephanite, bournonite, $CuPbSbS_3$, has the unit cell with space group symmetry $Pn2_1m$ and contains two crystallographically different Sb atoms in a unit cell: Sb (A) and Sb (B) (Fig. 2). Both Sb (A) and Sb (B) atoms form SbS_3 pyramids, which are connected via Cu or Pb atoms [7, 8].

† This paper material was selected at XV International Youth Scientific School "Actual problems of magnetic resonance and its application", Kazan, 22 – 26 October 2012. The paper was recommended to publication in our journal and it is published after additional MRSej reviewing.

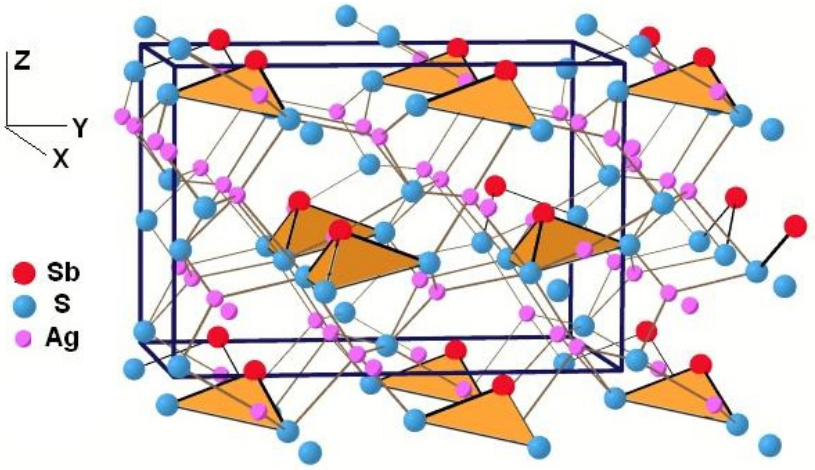

Figure 1. The crystal structure of stephanite Ag_5SbS_4. The trigonal pyramids SbS_3 are formed by the Sb atoms (at the only crystallographic position in the unit cell) surrounded by three S atoms. The figure was obtained with the BS Tools software [9].

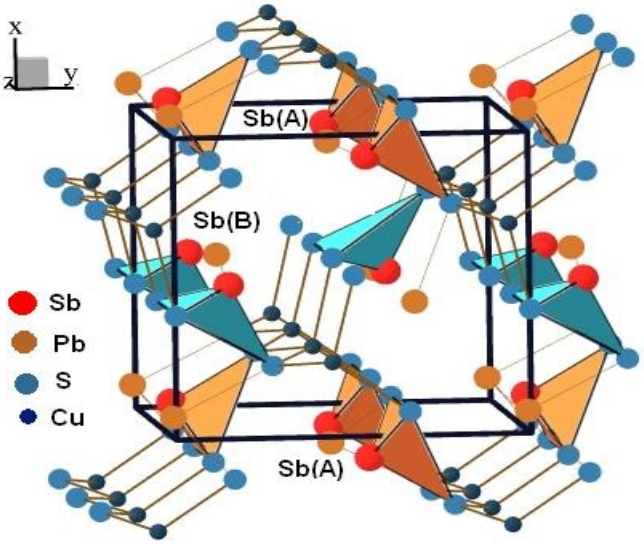

Figure 2. The crystal structure of bournonite $CuPbSbS_3$. The trigonal pyramids SbS_3 are formed by the Sb atoms surrounded by three S atoms. Two crystallographically different Sb (A) and Sb (B) positions are present. The figure was obtained with the BS Tools software [9].

3. Theoretical background of NQR

The Hamiltonian describing the interaction of the nuclear quadrupole moment eQ with the local electric field gradient (EFG) created by the on-site and surrounding electric charges can be written as [5]:

$$H_Q = \frac{eQV_{zz}}{4I(2I-1)}\left\{3I_z^2 - I(I+1) + 0.5\eta\left(I_+^2 + I_-^2\right)\right\}, \tag{1}$$

where V_{zz} is the largest component of the EFG tensor;

$$\eta = \frac{V_{xx} - V_{yy}}{V_{zz}} \tag{2a}$$

is the asymmetry parameter showing the deviation of the EFG symmetry from the axial one; the value of η lies in the range [0; 1].

The EFG components satisfy Laplace equation

$$V_{xx} + V_{yy} + V_{zz} = 0 . \tag{2b}$$

As follows from (2a) and (2b),

$$V_{yy} = -0.5(\eta + 1)V_{zz} , \tag{3a}$$

$$V_{xx} = 0.5(\eta - 1)V_{zz} . \tag{3b}$$

One of the goals of an NQR measurement is to determine the quadrupole coupling constant eQV_{zz} and the asymmetry parameter η, which contain information about the environment of the nucleus. The magnetic dipolar transitions obeying the usual magnetic dipole selection rule $\Delta m = \pm 1$ can be observed in the NQR experiment. The corresponding NQR frequencies depend on two parameters - eQV_{zz} and η. In the case $\eta \leq 0.2$, approximate dependences of the NQR frequencies on the asymmetry parameter are known [5]. For example, for $I = 7/2$:

$$\nu_{\pm 7/2 \leftrightarrow \pm 5/2} = \frac{3}{14} eQV_{zz}\left(1 - 0.099\eta^2 - 0.018\eta^4\right), \tag{4}$$

$$\nu_{\pm 5/2 \leftrightarrow \pm 3/2} = \frac{2}{14} eQV_{zz}\left(1 - 0.516\eta^2 + 1.048\eta^4\right), \tag{5}$$

$$\nu_{\pm 3/2 \leftrightarrow \pm 1/2} = \frac{1}{14} eQV_{zz}\left(1 + 3.429\eta^2 - 4.011\eta^4\right). \tag{6}$$

4. Experimental part

Two natural powder minerals, Ag_5SbS_4 and $CuPbSbS_3$, have been studied. Samples were kindly granted by the Geological Museum, Kazan Federal University. Phase homogeneity and structure were confirmed by X-ray diffraction analysis at room temperature. The NQR measurements were performed using ^{121}Sb nuclei (nuclear spin $I = 5/2$, natural abundance 57.25%, gyromagnetic ratio $\gamma/2\pi = 10.188$ MHz/T, nuclear quadrupole moment $Q = -0.543$ b) and ^{123}Sb nuclei ($I = 7/2$, 42.75%, $\gamma/2\pi = 5.517$ MHz/T, $Q = -0.692$ b). Pulsed NQR spectrometer with quadrature detection has been used.

5. Results and discussion

The ^{121,123}Sb NQR spectra of Ag_5SbS_4 and $CuPbSbS_3$ are shown in Fig. 3 [10]. The number of NQR lines is defined (i) by the amount of crystallographic nonequivalent positions of quadrupole nucleus in the crystal structure, (ii) by the magnitude of nuclear spin I and (iii) by the number of naturally available isotopes of quadrupole nucleus. Antimony has two abundant isotopes: ^{121}Sb (57.25%) with nuclear spin $I = 5/2$ and ^{123}Sb (42.75%) with nuclear spin $I = 7/2$. So, for $I = 5/2$ two NQR lines can be observed, corresponding to transitions $m_I = \pm 1/2 \leftrightarrow \pm 3/2$ and $\pm 3/2 \leftrightarrow \pm 5/2$. For $I = 7/2$ three NQR lines can be observed, corresponding to transitions $m_I = \pm 1/2 \leftrightarrow \pm 3/2$, $\pm 3/2 \leftrightarrow \pm 5/2$ and $\pm 5/2 \leftrightarrow \pm 7/2$. Thus, the single antimony crystal-chemical position in the structure of the material under study yields five NQR signals. The ^{121,123}Sb NQR spectrum for Ag_5SbS_4 consists of five lines (two lines for ^{121}Sb transitions and three lines for ^{123}Sb transitions), whereas ^{121,123}Sb NQR spectrum for $CuPbSbS_3$ contains ten lines. These results are in good agreement with the crystallographic data. The observed number of Sb NQR lines confirm that Ag_5SbS_4 has only one crystal-chemical site of antimony, but $CuPbSbS_3$ has two nonequivalent antimony positions.

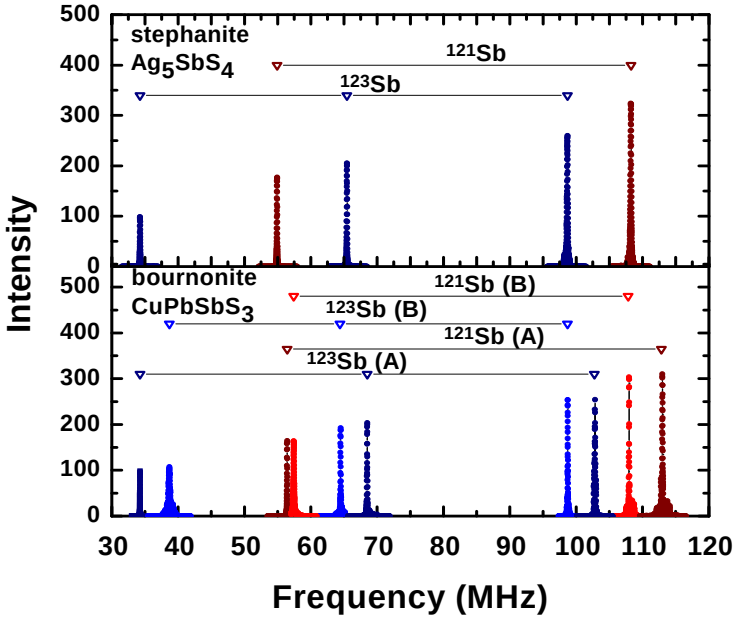

Figure 3. The ^{121,123}Sb NQR spectra of stephanite, Ag_5SbS_4, and bournonite, $CuPbSbS_3$. The number of NQR lines indicates that Sb atoms occupy only one crystallographic position in Ag_5SbS_4, whereas in $CuPbSbS_3$, two positions (referred to as A and B). For details, see text.

Stephanite

The temperature dependence of ^{123}Sb NQR frequency ν and NQR line-width $\Delta\nu$ for Ag_5SbS_4 are shown in Fig. 4 (transition $\pm1/2 \leftrightarrow \pm3/2$) [11]. Generally, the NQR frequency decreases with increasing temperature without any significant anomalies. According to the Bayer model, such behavior corresponds to the averaging of the EFG owing to a temperature-induced increase in the amplitude of lattice vibrations [12]. However, we point out the weak change of the slope in the temperature dependence of ν at about 140 K. NQR line-width, $\Delta\nu$, has similar behavior: $\Delta\nu$ decreases with increasing temperature. As one can see in details, there are two bends at 140 K and 250 K on the curve. It is important that the line-widths are not larger than 90 kHz at all temperatures. This rather small value signifies that stephanite represents a high-ordered structure though it is rather complex. More detailed information can be obtained from the temperature dependence of asymmetry parameter η and V_{xx} component of EFG (Fig. 5).

These parameters were calculated using formulas (3)-(6). In general, the value of η varies not much (about 10%). This indicates substantial, but not large distortions of umbrella-like SbS_3 complexes. As one can see, there is a distinct bend in the $\eta(T)$ curve at 140 K, and peculiarities in the behavior of the V_{xx} at about 80, 140, and 250 K. Thus, all parameters of the NQR spectra exhibit an anomalous temperature dependence. The bending character of the curves is typical for structural transformations of displacement type, which change the configuration of the local field, but do not change the symmetry. Thus, we can conclude that

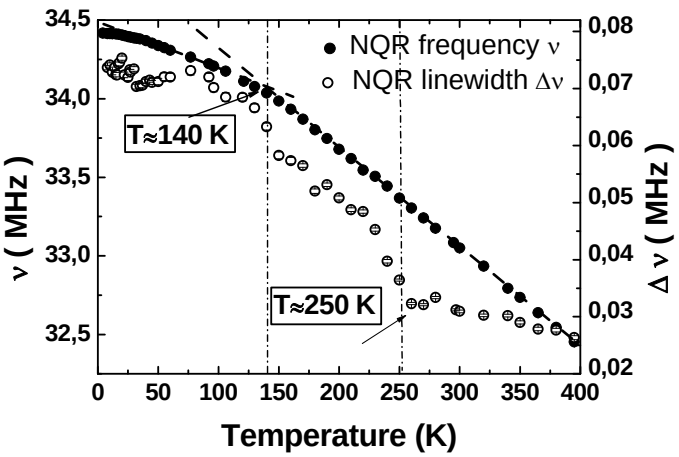

Figure 4. The temperature dependence of ^{123}Sb NQR frequency ν ($\pm1/2 \leftrightarrow \pm3/2$) and line-width $\Delta\nu$ in Ag_5SbS_4.

there is a structural transformation of SbS_3 complexes in Ag_5SbS_4 at 140 K [11]. Similar structural changes have been observed in compounds structurally related to stephanite: proustite Ag_3AsS_3 and pyrargyrite Ag_3SbS_3. Later it was found that these changes correspond to phase transitions of second order, which are accompanied by slight structural reorganizations of antimony coordination spheres, leading to the appearance of ferroelectric properties [13, 14].

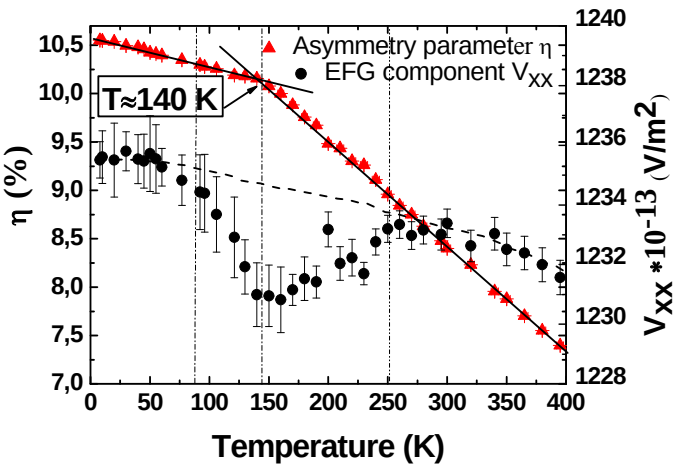

Figure 5. The temperature dependence of asymmetry parameter η and EFG V_{xx} component (^{123}Sb) in stephanite.

The temperature dependence of antimony nuclear spin-lattice relaxation rate, $1/T_1$, can be described very well by the expression $T_1^{-1}(T) = \alpha T^2 + \beta \exp(-E_a / T)$. The first term in this expression corresponds to the second order Raman process; second term reflects the presence of internal movements with the activation energy $E_a = 0.29$ eV. We suppose that the internal motions in Ag_5SbS_4 are due to the diffusion of silver ions over the crystal structure. This conclusion is confirmed by the theoretical estimations pointing out to silver ions diffusion [6]. Another evidence of Ag diffusion is narrowing of spectral line (Fig. 4) due to averaging of the EFG distribution by diffusion motion. Interestingly, ion conductivity due to movement of Ag ions was also experimentally observed in pyrargyrite Ag_3SbS_3 and proustite Ag_3AsS_3, with an activation energy of 0.4 and 0.42 eV, respectively [15].

Bournonite

The temperature dependence of ν for the both antimony positions in $CuPbSbS_3$ shows a normal Bayer behavior, as in the Ag_5SbS_4. However, in contrast to stephanite, no peculiarities in $\nu(T)$, $\eta(T)$ were revealed, which means that there are no prominent structural transitions in bournonite. However, analysis of spectroscopic parameters points to interesting crystal-chemical features of $CuPbSbS_3$.

The NQR frequencies ν and corresponding line-widths $\Delta\nu$ for both A and B positions in $CuPbSbS_3$ at $T = 77$ K are presented in Table 1. The values of quadrupole constant $eV_{zz}Q$ and asymmetry parameter η have been calculated from experimental data (using formulas (5)-(6)). The obtained values of the asymmetry parameter η for A and B antimony positions (0.5% and ≈ 22%) indicate the significant difference in the symmetry of the corresponding SbS_3 pyramids. The $Sb(A)S_3$ pyramid has the symmetry very close to axial, while $Sb(B)S_3$ is substantially distorted. It should be noted that the change in η with temperature is negligible for both positions. The average value of the quadrupole constant eQV_{zz} for both positions is about 470 MHz. However, stibnite Sb_2S_3, structurally related to $CuPbSbS_3$ compound, has the value of eQV_{zz}(^{123}Sb) about 297 MHz for the A position and 397 MHz for the B position [16]. Such difference can be explained by an increase of a Sb–S bond polarity caused by the fields created by metallic atoms (in $CuPbSbS_3$ case, Cu and Pb) [17].

Table 1. The NQR spectroscopic parameters in bournonite $CuPbSbS_3$ at 77 K.

Position	Transition	ν (MHz)	$\Delta\nu$ (kHz)	eQV_{zz} (MHz)	η (%)
A	^{123}Sb ±1/2 ↔ ±3/2	34.275(5)	35.5(5)	479.6(6)	0.5(1)
	^{123}Sb ±3/2 ↔ ±5/2	68.509(4)	62.3(4)		
B	^{123}Sb ±1/2 ↔ ±3/2	38.683(5)	210 ± 20	463.2(6)	21.8(5)
	^{123}Sb ±3/2 ↔ ±5/2	65.453(5)	60.0(5)		

The detailed shape of ^{123}Sb NQR spectral lines (transitions ±1/2 ↔ ±3/2) for the A and B positions in $CuPbSbS_3$ are shown in Fig. 6. As one can see, the NQR line-width of the B position is larger than that of the A position.

The NQR line-width is a good indicator of the degree of lattice perfection of a crystal under study. As follows from Eqs. (4)-(6), the NQR line-width is determined by the distribution ΔV_{zz} of the V_{zz} component of the EFG and the distribution of the asymmetry parameter $\Delta\eta$. For bournonite, ^{123}Sb NQR line-width is 35 kHz for the site A (transition ±1/2 ↔ ±3/2). This is a relatively small value for a natural mineral pointing to a high degree of structural order. However, Sb line-width is 250 kHz for the site B. This indicates that antimony atoms at the site B do not occupy a definite position with respect to their neighboring sulfur atoms in the $Sb(B)S_3$ complexes; in other words, their locations are distributed around the average position. Such distribution Sb is caused probably by lattice defects, different impurities embedded in the crystal. On the contrary, positions of the Sb(A) atoms are almost the same in all of the $Sb(A)S_3$ pyramids. Thus we can conclude that lattice defects are located irregularly and concentrated mainly in the vicinity of the $Sb(B)S_3$ complexes. This is typical feature for low-symmetry crystals having several nonequivalent atomic positions in the unit cell [16].

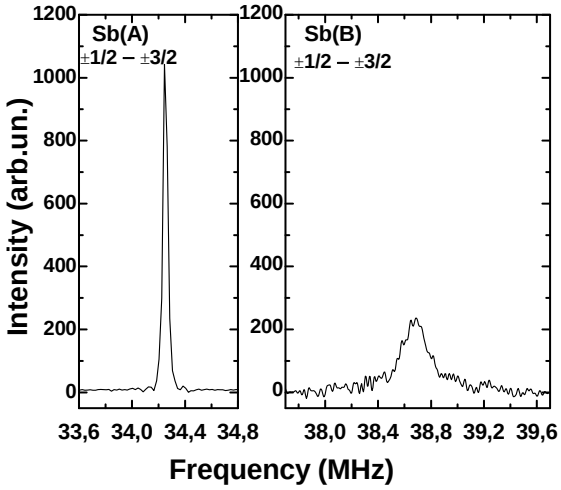

Figure 6. The ^{123}Sb NQR spectral lines for the positions A (left) and B (right) in $CuPbSbS_3$ at 77 K (transition ±1/2 ↔ ±3/2).

In addition, we performed calculations of ΔV_{zz} and $\Delta\eta$ contributions to the line-widths in conformity with [18]. It was found that $\Delta\nu/\nu \approx \Delta V_{zz}/V_{zz} \approx 10^{-3}$ for the Sb(A) position; i.e. $\Delta\nu$ is determined by the distribution of V_{zz} values. However, $\Delta\nu/\nu \approx \Delta\eta/\eta \approx 20\cdot10^{-3}$ for the Sb(B) position; in other words, the main contribution to broadening of Sb(B) NQR lines is the distribution of the asymmetry parameter η.

The degree of distortion of coordination polyhedra is defined by interatomic distances and valence angles. X-ray diffractometry tends to average atom positions over all unit cells, both perfect and distorted. Hence, geometrical parameters (interatomic distances and valence angles) can not be always defined within an appropriate accuracy. For instance, both of the SbS_3 polyhedra in bournonite are distorted in a similar manner, according to the X-ray analysis [7]. As it follows from our NQR data, sulfur from $Sb(A)S_3$ umbrella-like pyramids and more distant neighbors create almost axially symmetric EFG at Sb(A) site ($\eta = 0.5\%$), while the EFG symmetry at Sb(B) in $Sb(B)S_3$ complexes substantially deviates from axial ($\eta = 22\%$). Actually, it was found recently that the Sb–S distances in the A position are almost the same (2.464, 2.467, and 2.467 Å), while the Sb–S distances for the position B have different lengths (2.438, 2.463, and 2.463 Å) [8]. Our NQR spectroscopic results are in a good agreement with these recent studies. Thereby, high sensitivity of the NQR spectroscopy to crystal-chemical properties of solid state materials allows us to specify and correct the crystallographic data. More detailed studies of bournonite will be presented elsewhere.

6. Conclusions

Two natural minerals, stephanite and bournonite, have been investigated by ^{121,123}Sb NQR spectroscopy. The analysis of obtained experimental results demonstrates high sensitivity and accuracy of NQR to individual features of crystal structure of solids including the local symmetry, structural phase transition and transport properties.

References

1. Dittrich H., Stadler A., Topa D., Schimper H.J., Basch A. *Phys. Status Solidi A* **206**, 1034 (2009)
2. Bindi L., Evani M., Menchetti S. *Acta. Cryst. B* **62**, 212 (2006)
3. Orlova A.Yu., Gainov R.R., Dooglav A.V., Pen'kov I.N., Mozgova N.N. *Magn. Reson. Solids* **10**, 6 (2008)
4. Platova T.A., Mukhamedshin I.R., Alloul H., Dooglav A.V., Collin G. *Phys. Rev. B* **80**, 224106 (2009)
5. Grechishkin V.S. *Nuclear Quadrupole Interactions in Solid*, Nauka, Moscow (1973) (*in Russian*)
6. Leitl M., Pfitzner A., Bindi L. *Mineralogical Magazine* **73**, 17 (2009)
7. Edenharter A., Nowacki W., Takeuchi Y., *Z. Kristallogr*. **131**, 397 (1970)
8. Kharbish S., Giester G., Beran A. *N. Jb. Miner. Abh.* **187**, 159 (2010)
9. Ozawa T.C., Kang S.J. *J. Appl. Cryst.* **37**, 679 (2004)
10. Gainov R.R., Dooglav A.V., Vagizov F.G., Pen'kov I.N., Golovanevskiy V.A., Orlova A.Yu., Evlampiev I.A., Klekovkina V.V., Klingelhöfer G., Ksenofontov V., Mozgova N.N. *European journal of mineralogy* [submitted]
11. Orlova A.Yu., Gainov R.R., Dooglav A.V., Pen'kov I.N., Korolev E.A. *JETP Letters* **96**, 370 (2012)
12. Bayer H. *Z. Physik* **130**, 227 (1951)
13. Baisa D.F., Bondar A.V., Gordon A.Ya. *Ferroelectrics* **20**, 219 (1978)
14. Abdullin R.S., Pen'kov I.N., Nizamutdinov R.M., Grigas I., Safin I.A. *Fizika Tverdogo Tela* **19**, 1632 (1977) (*in Russian*)
15. Schonau K.A., Redfern S.T. *J. Appl. Phys*. **92**, 7415 (2002)
16. Pen'kov I.N., Safin I.A. *Int. Geol. Review* **9**, 793 (1967)
17. Pen'kov I.N., Safin I.A. *Dokl. Akad. Nauk SSSR* **161**, 1404 (1965) (*in Russian*)
18. Bryant P.J., Hacobian S. *J. Mol. Structure* **83**, 311 (1982)